EURASIAN JOURNAL OF MATHEMATICAL AND COMPUTER APPLICATIONS
ISSN 2306–6172
Volume 13, Issue 1 (2025) 108–117

SIMULATION OF GAS DISCHARGE IN A HELIUM BUBBLE IN LIQUID DIELECTRIC

Savenko R. A. , Karpov D. I. [1], Ridel A. V. , Korobeynikov S. M.

Abstract 3D simulation of the initial stage of the development of gas discharge in a helium bubble in dielectric liquid between flat electrodes has been performed with the use of a diffusion-drift approximation. The values of the electric field in the bubble and on its surface were obtained before and after the electrons reached the bubble boundary. The electric field strength increased from 48 kV/cm to 79 kV/cm at the pole of the bubble closest to the anode. Data on discharge characteristics at the initial stage within the framework of the considered model are obtained: plasma concentration, distribution and evolution over time of concentrations of positive helium ions and electrons. The charge distribution at the bubble boundary closest to the anode is calculated.

Key words: partial discharge, gas discharge, "true" charge, 3D simulation, parallel computing.

AMS Mathematics Subject Classification: 78-10, 65Z05.

DOI: 10.32523/2306-6172-2025-13-1-108-117

1 Introduction

The electrical breakdown of a liquid dielectric occurs due to the development of a system of plasma channels in the liquid, connecting electrodes of different polarities [1, 2]. The system of these channels is called streamers. To date, it is impossible to say that the mechanisms of formation of such channels in liquids are clear. In the case when channels develop from the electrode surface, near-electrode processes can play an essential role [3]. This complicates the study of the mechanisms of channel formation. In [4, 5], the phenomenon of the formation of streamers from the surface of a bubble floating freely in a dielectric liquid after a partial discharge (PD) in the bubble was discovered and investigated. A partial discharge leads to charging of the gas bubble-liquid interface and a significant increase in the electric field at the poles of the bubble relative to the average electric field in the discharge gap [4, 6]. In this case, the influence of near-electrode processes is excluded and we can talk about "pure" mechanism of channel formation in the liquid. In this case, the initiation of the streamer will depend only on the local electric field strength in the liquid on the surface of the bubble. Thus, the task of determining the distribution of the electric charge and, accordingly, the local electric field over the surface of the bubble after the PD in it is important.

[1]Corresponding Author.

To date, there are no experimental methods that would directly measure the electric field at the pole of the bubble immediately after the PD in it. Therefore, a special role is played by the possibility of calculating the characteristics of the PD and, then, the conditions for the formation of streamers from the surface of the bubble. In [6], calculations of the electric field strength and the distribution of the "true" charge on the surface of the bubble after the PD were performed, assuming that the entire volume of the bubble is a homogeneous conductor during partial discharge. Obviously, these calculations require revision, since it does not take into account the shape of the ionization wave in the gas when it reaches the bubble boundary. Accordingly, the surface distribution of the "true" charge and field differ from those obtained in [6]. In this paper, an attempt is made to describe in more detail the PD process in a helium bubble, experimentally investigated in [4, 5, 7, 8]. A numerical simulation of the development of electron avalanches from the initiating seed at PD in a bubble in a dielectric at the initial stages of the process is performed. To do this, a three-dimensional numerical model was implemented that allows parallel calculations to be performed on graphics accelerators (GPUs). The features of the development of the ionization wave, its reach of the bubble boundary, and the calculation of the distribution of free electric charges on the surface and the corresponding electric field are studied.

2 Physical model

As experiments [7, 8] show, the development of a partial discharge in a 1-2 mm bubble in a liquid dielectric takes $50 - 70$ ns. The hydrodynamic time in this case is 0.7-1.4 microseconds (at the speed of sound in transformer oil about 1400 m/s). Therefore, in calculations of the development of ionization processes, it is possible to neglect the deformation of the bubble during the PD, despite the fact that experiments often observe the stretching of the bubble along the electric field after the PD. Estimates show that during the development of avalanches in the bubble, the displacement current density is much less than the conduction current and the electric field considered to be potential field. In addition, the influence of the magnetic field on the dynamics of electrons is several orders of magnitude less than the influence of the electric field at the initial stage of discharge development. Therefore, the magnetic field was excluded from Maxwell's equations.

To solve the problem of the development of the electronic avalanche, the following system of equations was used

$$\begin{aligned} \nabla(\varepsilon_0\varepsilon\nabla(\varphi)) &= -|e|(n_+ - n_e), \\ \frac{\partial n_+}{\partial t} + \nabla(\mu_+ n_+ \mathbf{E}) &= \nabla(D_+\nabla n_+) + \alpha\,|\mu_e n_e \mathbf{E} + D_e\nabla n_e| - \beta n_+ n_e - \gamma n_+ n_e^2, \\ \frac{\partial n_e}{\partial t} - \nabla(\mu_e n_e \mathbf{E}) &= \nabla(D_e\nabla n_e) + \alpha\,|\mu_e n_e \mathbf{E} + D_e\nabla n_e| - \beta n_+ n_e - \gamma n_+ n_e^2, \end{aligned} \quad (1)$$

The first equation of the system is the Gauss theorem for dielectrics. The following designations are used: ε is the relative dielectric permittivity of a substance ($\varepsilon = 1$ in gas), ε_0 is the electrical constant, φ is the electric field potential, e is the electron charge, n_+ is the concentration of positively charged ions, n_e is the electron concentration.

The second and third equations are continuity equations for the concentrations of electrons and positive ions, where the following designations are adopted: μ_+ is the mobility of positive ions, μ_e is the mobility of electrons, $\mathbf{E}$ is the electric field strength, D_+ is the diffusion coefficient of positive ions, D_e is the electron diffusion coefficient, α is the impact ionization coefficient, β is the two-particle recombination coefficient, γ is the three-particle recombination coefficient. The model assumes that the ionization coefficient, the electron mobility, and the electron diffusion coefficient depend on the local electric field.

The ionization term in the form of the product of the electron flux modulus and the ionization coefficient is taken from [9].

The following boundary conditions were used for the first equation of the system (1). For flat anode and cathode (sides 1 and 2 of the simulation region in Fig. 1) the electric field potential was set as

$$\varphi = V_0, \quad \text{anode}, \qquad \varphi = 0, \quad \text{cathode}. \tag{2}$$

Here V_0 is the applied voltage. For the side walls of the simulation region the linear change of the electrical potential from V_0 to 0 was supported during simulations. Usual boundary conditions were fulfilled at the bubble-liquid interface

$$\varepsilon(\nabla\varphi)_{n2} - (\nabla\varphi)_{n1} = -|e|(n_{s+} - n_{se})/\varepsilon_0, \qquad (\nabla\varphi)_{\tau 2} = (\nabla\varphi)_{\tau 1}. \tag{3}$$

Here the index 2 is referred to liquid dielectric, index 1 is reffered to a gas bubble, n_{s+} and n_{se} are the surface number densities of the positive charges and electrones on the bubble wall, respectively. The indexes n and τ denote the projections of the electric field vector on normal and tangential directions to the boundary between different substances, correspondingly. The dielectric permittivity of helium inside bubble is taken to be equal to 1.

The transport equations (the second and the third equations in (1)) for positive ions and electrons were solved inside the bubble only (region 3 in Fig. 1). The non-flux condition was used for the total flux (due to mobility in the electric field and diffusion) of positive ions $\mathbf{J}_+$ on the bubble wall as well as for the total flux of electrons $\mathbf{J_e}$

$$J_{+n} = ((\mu_+ n_+ \mathbf{E} - \mathrm{D_+}\nabla \mathrm{n_+}), \mathbf{n}) = 0, \qquad \mathrm{J_{en}} = ((-\mu_\mathrm{e} \mathrm{n_e}\mathbf{E} - \mathrm{D_e}\nabla \mathrm{n_e}), \mathbf{n}) = 0. \tag{4}$$

Here $\mathbf{n}$ is the external normal vector to the bubble surface.

No ionization of the dielectric molecules or possible chemical processes on the bubble wall were considered.

The system of equations (1) – (4) was solved numerically as described below. First, the distribution of the electric field potential was calculated in the simulation region without free charges (only dielectric and gas bubble). This distribution was considered as initial condition for the following dynamics. Then, a small spherical electrically neutral seed of positive ions and negative electrons was placed to the bubble. The uniform distributions for positive charges and for electrons were used in the seed. The seed was placed at different distances from bubble center at different simulations. Then the evolution of the electron avalanches in helium in the bubble was calculated step by step. The distribution of the electric field potential was recalculated at every time step in order to take into account the changes in the charge densities.

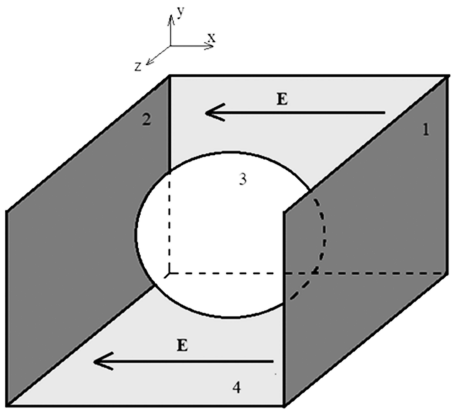

Figure 1: The scheme of the calculation region. 1 - anode, 2 - cathode, 3 - gas bubble, 4 - side walls.

3 Numerical model

The region of calculations is shown in Fig. 1 and consisted of $258 \times 258 \times 258$ grid nodes, the grid step was equal to 12 microns. A part of the calculation region in the center having the spherical shape imitated a gas bubble. The diameter of the bubble was 1.8 mm, which corresponds to 154 grid nodes. On the axis of symmetry of the bubble along the direction of the electric field, the seeds of electrons and positive ions were given in the form of balls with a radius of 8 nodes, each with an average concentration of $4 \cdot 10^6$ m^{-3}, while the total charge was zero. The potential was calculated using simple iterations with a parallel algorithm implemented on a graphics accelerator. This made it possible to significantly reduce the simulation time while maintaining high accuracy in calculating the potential. Parallel calculations were performed on an NVIDIA Titan Black graphics card with 2880 computing cores. The distribution of the electric field in a bubble and a dielectric without free charges with a relative error of less than 10^{-11} was calculated as initial conditions. Then, at each time step at the beginning of the simulation, 5000 iterations were required to maintain the initial accuracy. Further, the number of iterations had to be increased from step to step so that the relative error of the calculations was at least 10^{-10}. After calculating the potential, the electric field strength in the region of calculations was obtained.

When calculating concentrations, the values of the mobility of positive ions μ_+, the diffusion coefficient of positive ions D_+, the coefficient of two-particle recombination β and three-particle recombination γ were assumed to be constant and equal to 0.001 m^2/(V s), $2.5 \cdot 10^{-5}$ m^2/s, 10^{-13} m^3/s and 10^{-31} m^6/s, respectively. The impact ionization coefficient was taken from the experimental data of [10, 11, 12, 13], which were approximated by the following piecewise continuous function

$$\alpha(E) = \begin{cases} 0, & |\mathbf{E}| < 2 \ \frac{\text{kV}}{\text{cm}}, \\ 0.472|\mathbf{E}|^{2.15}\text{cm}^{-1}, & 2\frac{\text{kV}}{\text{cm}} < |\mathbf{E}| \leq 50 \ \frac{\text{kV}}{\text{cm}}, \\ 771|\mathbf{E}|^{0.25}\text{m}^{-1}, & 50\frac{\text{kV}}{\text{cm}} < |\mathbf{E}| \leq 2 \ \frac{\text{MV}}{\text{cm}}, \\ 510^3 \ \text{m}^{-1}, & |\mathbf{E}| > 2, \ \frac{\text{MV}}{\text{cm}}. \end{cases}$$

The experimental data on the mobility of electrons in helium μ_e from [14, 15] were

approximated by the following dependence

$$\mu_e = \begin{cases} 8000\frac{\text{cm}^2}{\text{V s}}, & |\mathbf{E}| \le 0.01\frac{\text{kV}}{\text{cm}}, \\ 1001|\mathbf{E}|^{-0.45\,\frac{\text{cm}^2}{\text{V s}}}, & 0.01\frac{\text{kV}}{\text{cm}} < |\mathbf{E}| \le 1\frac{\text{kV}}{\text{cm}}, \\ 1000\frac{\text{cm}^2}{\text{V s}}, & |\mathbf{E}| > 1\frac{\text{kV}}{\text{cm}}. \end{cases}$$

Similarly, based on the experimental data from [12, 14, 15], an approximation of the dependence of the electron diffusion coefficient D_e on the electric field strength was used in the form

$$D_e = \begin{cases} 200\frac{\text{cm}^2}{\text{s}}, & |\mathbf{E}| \le 0.1\frac{\text{kV}}{\text{cm}}, \\ 1580|\mathbf{E}|^{0.9\,\frac{\text{cm}^2}{\text{s}}}, & |\mathbf{E}| > 0.1\frac{\text{kV}}{\text{cm}}. \end{cases}$$

A conservative explicit scheme was used to solve system (1). The use of an implicit scheme in this task led to a number of difficulties. Firstly, it is problematic to formulate the fully implicit scheme because of the non-linear dependence of the transport coefficients on the lacal electric field value. Secondly, in the case of an "half-implicit" scheme we applied, test calculations for 1D, 2D and 3D cases always led to a violation of the conservation of full charge after the ionization wave reached the bubble-liquid dielectric boundary. The error in the value of the full charge reached more than 10%. Third, after the ionization wave reached the bubble wall, a charge accumulated on the wall, and in the case of an our "half-implicit" schemes, negative electron concentrations were observed in some cells close to the bubble boundary. These oscillations also reached large values comparable to positive concentration values.

In the numerical implementation of equations (1), the most important is the choice of finite-difference schemes for the terms of transfer and diffusion, since it is these approximations that determine the stability of the scheme.

The transfer term in calculating concentrations was approximated by a finite-difference upstream explicit scheme, an example of approximating the transfer operator $A^{ex}_{i,j,k}$ for the derivative along the axis x from the equation on electron concentrations has the form

$$A^{ex}_{i,j,k} = F^{ex}_{i+1,j,k} - F^{ex}_{i,j,k}, \quad F^{ex}_{i,j,k} = \begin{cases} \mu_{e\,i-1/2,j,k} n_{e\,i,j,k} \frac{\varphi_{i-1,j,k} - \varphi_{i,j,k}}{h}, & \varphi_{i,j,k} > \varphi_{i-1,j,k}, \\ \mu_{e\,i-1/2,j,k} n_{e\,i-1,j,k} \frac{\varphi_{i-1,j,k} - \varphi_{i,j,k}}{h}, & \varphi_{i,j,k} \le \varphi_{i-1,j,k}. \end{cases}$$

where $F^{ex}_{i,j,k}$ is the flux of electrons into the cell, in the center of which there is a node with coordinates (i, j, k), $\mu_{e\,i-1/2,j,k}$ is the value of electron mobility at a point $(i-1/2, j, k)$, that is calculated for the value of the electric field $E_{i-1/2,j,k} = (\varphi_{i-1,j,k} - \varphi_{i,j,k})/h$, h is the grid step. For positive ions, the mobility coefficient μ_+ was considered constant and the conditions for the flux were reversed.

The diffusion term was approximated by a 3-point explicit finite-difference scheme, an example of a difference operator $B^{ex}_{i,j,k}$ for an x-axis component for electrons has the form

$$B^{ex}_{i,j,k} = D^{ex}_{i+1/2,j,k} \frac{n_{e\,i+1,j,k} - n_{e\,i,j,k}}{h} - D^{ex}_{i-1/2,j,k} \frac{n_{e\,i,j,k} - n_{e\,i-1,j,k}}{h},$$

where $D^{ex}_{i+1/2,j,k}$ is the value of the electron diffusion coefficient at a point $(i+1/2, j, k)$. For positive ions, the diffusion coefficient D_+ is constant, so the diffusion flux of positive ions is proportional to the second derivative of the concentration along the coordinate, which was also approximated on a three-point central difference template.

The approximation of the boundary conditions for charge' fluxes was carried out by analogy with the numerical scheme proposed in [16]. For example, the contribution to

the electron concentration at the boundary node i_b (node $i_b - 1$ belongs to the bubble and node $i_b + 1$ is in liquid dielectric) on the bubble wall because of the fluxes along only x direction was calculated as

$$n^{p+1}_{e\ i_b,j,k} = n^{p}_{e\ i_b,j,k} - \mu_{e\ i_b-1/2,j,k}\ n^{p}_{e\ i_b-1,j,k} \frac{\varphi_{i_b-1,j,k} - \varphi_{i_b,j,k}}{h} - D_{e\ i_b-1/2,j,k} \frac{n^{p}_{e\ i_b,j,k} - n^{p}_{e\ i_b-1,j,k}}{h} - \beta n^{p}_{+} n^{p}_{e} - \gamma n^{p}_{+} (n^{p}_{e})^2,$$

where p is the current time step. After the calculation of the contribution of the x-flux to the concentration in boundary nodes we calculated the contributions of $y-$ and $z-$ fluxes, analogously.

The stability of this explicit scheme was ensured by choosing the time step τ at each step of the simulation. In this numerical scheme, two stability criteria must be taken into account: for the diffusion term and for the term responsible for the transfer. The large values of electric field strengths result in the situation that the estimate of the time step limitation due to diffusion turns out to be obviously less strict than the time step limitation due to transfer. Therefore, the stability of the scheme used in this work was determined only by the stability of the part describing the transfer. Taking into account the dependence of the electron mobility coefficient on the current electric distribution, a modified stability criterion was chosen, depending on the grid step h and the magnitude of the local field: $\tau \leq h/|E|^{1.1}_{\max}$

It was shown in a series of numerical experiments that such a criterion ensures the stability of the scheme used for all parameters of interest in our simulations.

4 Results and discussion

According to calculations, the characteristic time for electrons to reach the bubble boundary is 0.3-0.5 ns. When the electron wave front reached the boundary, an increase in the value of the electric field on the surface of the bubble was observed from a value of 47.6 kV/cm to 79.3 kV/cm. The change over time in the concentrations of charged particles and the electric field strength along the central axis is shown in Fig. 2 and Fig. 3, respectively. The velocity of the electron wave to the boundary was ~ 1000 km/s.

After the electrons reached the bubble boundary, data on electron concentrations on the bubble surface were recorded. The distributions of the surface electron density at the bubble-liquid dielectric boundary at different time points up to 1 ns from the moment of initiation are obtained. Fig. 4 shows a graph of the change in the surface density of electrons on the surface of the bubble along the direction y (or z). The ledges on the graph are related to the discreteness of the grid. In general, the dynamics of partial discharge is described as follows. During 0.32-0.36 ns, the electric field strength inside the bubble practically does not change, while the concentration of charges of both signs increases by about 10 orders of magnitude. Then, when the electron concentration exceeded the value of 10^{17} m^{-3}, a decrease in the electric field (shielding) in the central part of the bubble began. In this region, the total charge density is precisely zero, that is, the concentrations of electrons and positive ions are approximately equal. The shielded region first appears in the central part on the axis of symmetry of the bubble. Then it elongates into a cylinder of approximately constant cross-section with a radius

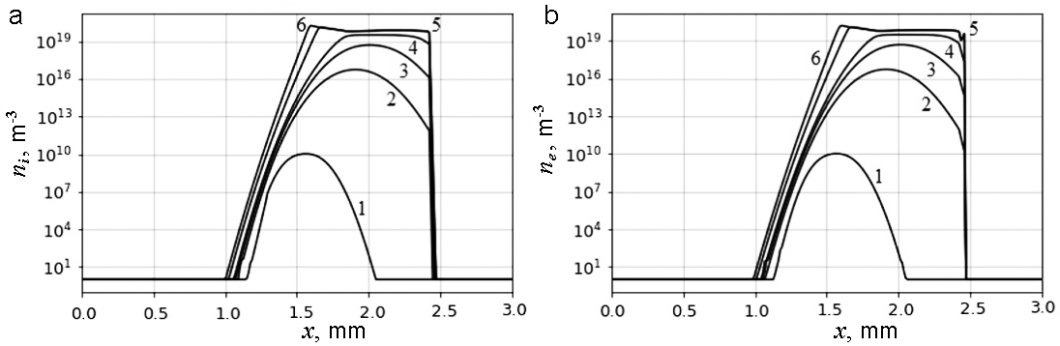

Figure 2: Concentrations of positive ions (a) and electrons (b) in the central section along the axis on a logarithmic scale at different time points: 1 пїS- 0.1 ns, 2 пїS- 0.3 ns, 3 пїS- 0.36 ns, 4 пїS- 0.4 ns, 5 пїS- 0.5 ns, 6 пїS- 0.56 ns.

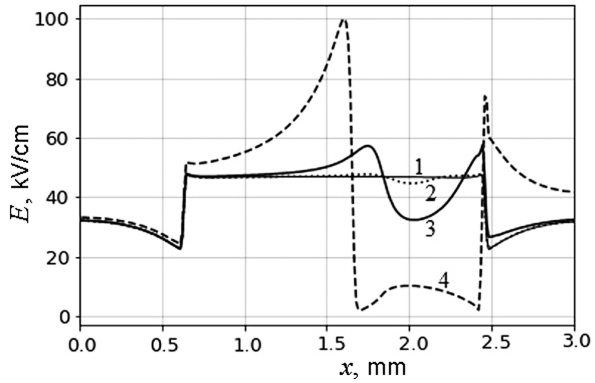

Figure 3: The electric field along a straight line parallel to the x axis and passing through the center of the bubble at different points in time. Thin solid line 1 пїS- 0.1 ns, dotted line 2 пїS- 0.36 ns, solid line 3 -пїS 0.4 ns, dotted line 4 пїS- 0.5 ns.

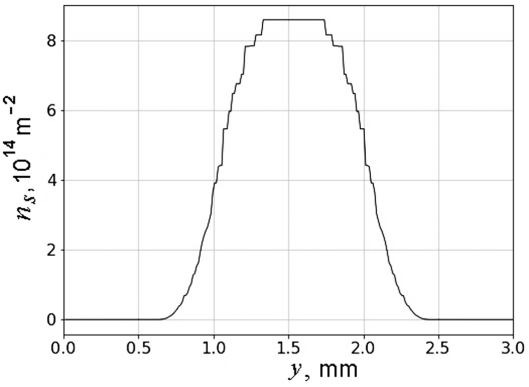

Figure 4: Distribution of the surface density of electrons on the surface of the bubble along y coordinate.

of 0.42 mm, parallel to the lines of the external electric field. Then, this cylinder is extended along the field to the bubble boundary following the electron front (Fig. 5). The moment at which the decrease in the field becomes noticeable can be considered as the moment of formation of a partial discharge plasma. Shielding led to a drop in field

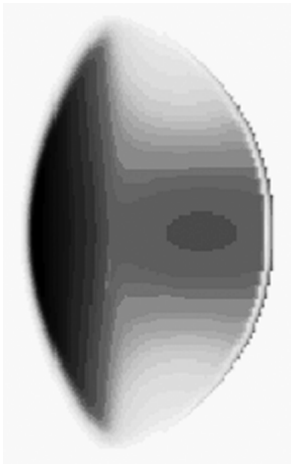

Figure 5: Distribution of the absolute value of the electric field at a time of 0.6 ns. Darker areas correspond to a lower field strength. A discrete bubble boundary is visible on the right. The dark bridge between the bubble boundary and the dark spherical surface is an area of weak shielding.

strength from values of about 48 kV/cm to 2 kV/cm near the bases of the cylinder and up to 10 kV/cm in the center of the cylinder (Fig. 3), while the plasma concentration in the shielded area reached 1-3 10^{20} m^{-3}.

In Figs. 3 and 5, the highest maximum of the electric field corresponds to the region of maximum positive electric charge, that is, the region of predominance of ion concentration. This positive charge front is usually formed at a distance of about 600 microns from the seed. It should be noted that a sharp change in the field strength in this area strongly affects the time step that ensures the stability of the numerical scheme. For example, for curve 2, the time step was 10^{-13} seconds, and for curve 4 it was already 10^{-16} seconds. A time step of less than 10^{-15} seconds makes calculations very problematic, since with such a small step, the time for full calculation becomes very long.

The results obtained give us more accurate infomation about charge distribution on the surface of a gas bubble in the process of PD in the bubble in comparizon to the model of uniform bubble conductivity used in [6]. In particular, we may observe the higher concentration of electrons to the bubble axis because of the shape of the ionization wave that occupies mainly the centra region of the bubble around the axis. The maximal electric field on the bubble apex is somewhat higher then in the case of the uniform conductivity modelof the bubble. Nevertheless, general conclusion about possible mechanism of streamer formation from the bubble surface after PD in the bubble made in [6] remains the same. The fields obtained in our calculations can provide only the conditions for the development of electrohydrodynamic instability of the charged bubble-liquid interface obtained in the works [17, 18] and in more general form in [19]. All other mechanisms (like the direct ionization of liquid molecules by electron impact etc.) look much less plausible.

4 Conclusion

In this paper, the parameters of the initial stage of a partial discharge in a gas bubble in a liquid dielectric are estimated. According to the simulation results, an increase in the modulus of the maximum local electric field by 1.67 times at the bubble boundary is observed. The distribution of electrons over the surface of the bubble (the distribution of the "true" charge) is obtained. According to calculations, the charge on the surface is not localized at the bubble pole closest to the anode, but is distributed over the entire half of the bubble surface closer to the anode.

Acknowledgement

The work is supported by Russian Science Foundation (RScF grant No. 22-79-10198).

References

[1] Kolb J.F., Joshi R.P., Xiao S., Schoenbach K.H., *Streamers in water and other dielectric liquids*, J. Phys. D: Appl. Phys., Vol. 41 (2008), 234007 (22p). DOI:10.1088/0022-3727/41/23/234007

[2] Liu Q., Xiang J., Wang Z., Lesaint O., *Streamer and Breakdown Characteristics of Dielectric Liquids Under Impulse Waveforms With Different Tail-Times*, IEEE Transactions on Dielectrics and Electrical Insulation, Vol. 29 No. 3 (2022), p. 1103пїS1110. DOI:10.1109/TDEI.2022.3173502

[3] Zhakin A.I. *Electrode and transient processes in liquid dielectrics*, Physics–Uspekhi, Vol. 49 Issue 3 (2006), p. 275пїS295. DOI:10.1070/PU2006v049n03ABEH002012

[4] Korobeynikov S., Ovsyannikov A., Ridel A., Karpov D., Lyutikova M., Kuznetsova Yu., Yassinskiy V., *Study of partial discharges in liquids*, Journal of Electrostatics, Vol. 103 (2020), art. 103412. https://doi.org/10.1016/j.elstat.2019.103412

[5] Korobeynikov S. M., Ridel A.V., Ovsyannikov A.G.,пїSKarpov D.I., Lyutikova M.N., Loman V.A., Savenko R.A., *Streamers in transformer oil initiated by partial discharge in a bubble at low AC electric fields*,пїSElectrical Engineering, Vol. 106 (2024), p. 5219пїS5228. DOI:10.1007/s00202-024-02359-y

[6] Karpov D. I., Ridel A. V., Savenko R. A., Korobeynikov S. M., *Initiation of a streamer in a liquid from the surface of a bubble in which a partial discharge occur*, Eurasian Journal of Mathematical and Computer Applications, Vol. 11 Issue 3 (2023), p. 63пїS75. DOI:10.32523/2306-6172-2023-11-3-63-75

[7] Korobeynikov S.M., Ridel A.V., Medvedev D.A., Karpov D.I., Ovsyannikov A.G., Meredova M.B. , *Registration and simulation of partial discharges in free bubbles at AC voltage*, IEEE Transactions on Dielectrics and Electrical Insulation, Vol. 26, Issue 4 (2019), p. 1035пїS1042. DOI:10.1109/TDEI.2019.007808

[8] Korobeynikov S., Ridel A., Karpov D., Ovsyannikov A., Meredova M., *Mechanism of partial discharges in free helium bubbles in transformer oil*, IEEE Transactions on Dielectrics and Electrical Insulation, Vol. 26 Issue 5 (2019), p. 1605пїS1611. DOI:10.1109/TDEI.2019.008199

[9] Kurbanismailov V.S. Omarov O.A., Ragimkhanov G.B., Tereshonok D.V., *Features of the formation and development of ionization fronts in a pre-ionized gas environment*, Pisma v ZhTF, Vol. 43 Issue 17 (2017), p. 73пїS81. DOI:10.21883/PJTF.2017.18.45036.16844

[10] Davies D.K., Jones F.L., Morgan C.G. *Primary ionization coefficient of helium*, Proceeding of the Physical Society, Vol. 80 Issue 4 (1962), p. 898пїS908. DOI:10.1088/0370-1328/80/4/312

[11] Ran J., Luo H., Yue Y., Wang X., *Measurement of the first TownsendпїSs ionization coefficients in helium, air, and nitrogen at atmospheric pressure*, Journal of Physical Society of Japan, Vol 83 (2014), p. 074503. DOI:10.7566/JPSJ.83.074503

[12] Smirnov B.M. *Physics of ionized gases*, John Wiley & Sons, Inc., 2001.

[13] Drawin H.W., Emard F., *Collisional-radiative volume recombination and ionization coefficients for quasi-stationary helium plasmas*, Z. Physik., Vol. 243 (1971), p. 326пїS340. https://doi.org/10.1007/BF01395918

[14] Biberman L.M., Vorobyev V.S., Yakubov I.T. *Kinetics of nonequilibrium low-temperature plasma*. Moscow: Nauka, 1982. (in Russian)

[15] Lakshminarasimha C.S., Lucas J., *The ratio of radial diffusion coefficient to mobility for electrons in helium, argon, air, methane and nitric oxide*, J. Phys. D: Appl. Phys., Vol. 10 (1977), p. 313пїS321. DOI:10.1088/0022-3727/10/3/011

[16] Ostapenko V.V., *Numerical simulation of wave flows caused by a shoreside landsacpe*, J. Appl. Mech. Tech. Phys., Vol. 40 No. 4 (1999), p. 647-654. https://doi.org/10.1007/BF02468439

[17] Zaitsev V. M., Shliomis M. I., *The aspect of interface instability between two liquids in a constant field*, Doklady Akademii Nauk SSSR, Vol. 188 Issue 6 (1969), p. 1261пїS1262.

[18] Grigoriev A. I., Grigoriev O. A., Shiryaeva S. O., *Mechanism of instability development of charged liquid surface* , Technical Physics, Vol. 62 Issue 9 (1992), p. 12пїS21.

[19] Zhakin A.I., *Electrohydrodynamics of charged surfaces*, Physics–Uspekhi, Vol. 56 Issue 2 (2013), p. 141пїS163. DOI:10.3367/UFNe.0183.201302c.0153

Savenko Roman Alexandrovich,
Lavrentyev Institute of Hydrodynamics
of SB RAS,
Lavrentyev av. 15, Novosibirsk, 630090, Russia
Novosibirsk State Technical University,
Karl Marx av. 20, 630090 Novosibirsk, Russia,
Email: savenko@hydro.nsc.ru,

Karpov Denis Ivanovich,
Lavrentyev Institute of Hydrodynamics
of SB RAS,
Lavrentyev av. 15, 630090 Novosibirsk, Russia
Novosibirsk State Technical University,
Karl Marx av. 20, 630090 Novosibirsk, Russia,
Email: karpov@hydro.nsc.ru,

Ridel Alexander Victorovich,
Novosibirsk State Technical University,
Karl Marx av. 20, 630090 Novosibirsk, Russia,
Email: ridel@corp.nstu.ru,

Korobeynikov Sergey Mironovich,
Novosibirsk State Technical University,
Karl Marx av. 20, 630090 Novosibirsk, Russia,
Email: korobeynikov@corp.nstu.ru.

Received 20.08.2024 , Accepted 15.01.2025, Available online 31.03.2025.